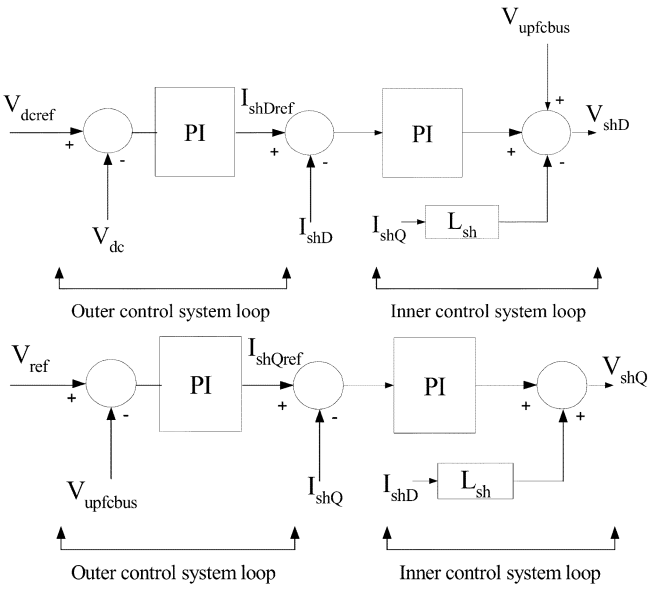

Fig. 1. De-coupled D-Q axis shunt converter control system.

II. Control Strategy for UPFC

A. Shunt Converter Control Strategy

The shunt converter of the UPFC controls the UPFC bus voltage/shunt reactive power and the dc link capacitor voltage. In this case, the shunt converter voltage is decomposed into two components. One component is in-phase and the other in quadrature with the UPFC bus voltage. De-coupled control system has been employed to achieve simultaneous control of the UPFC bus voltage and the dc link capacitor voltage.

B. Series Converter Control Strategy

The series converter of the UPFC provides simultaneous control of real and reactive power flow in the transmission line. To do so, the series converter injected voltage is decomposed into two components. One component of the series injected voltage is in quadrature and the other in-phase with the UPFC bus voltage. The quadrature injected component controls the transmission line real power flow. This strategy is similar to that of a phase shifter. The in-phase component controls the transmission line reactive power flow. This strategy is similar to that of a tap changer.

III. Basic Control System

A. Shunt Converter Control System

Fig. 1 shows the de-coupled control system for the shunt converter. The D-axis control system controls the dc link capacitor voltage $(V_{\rm dc})$ and the Q-axis control system controls the UPFC bus voltage $(V_{\rm upfcbus})$/shunt reactive power.

The details of the de-coupled control system design can be found in [16], [17]. The de-coupled control system has been designed based on linear control system techniques and it consists of an outer loop control system that sets the reference for the inner control system loop. The inner control system loop tracks the reference.

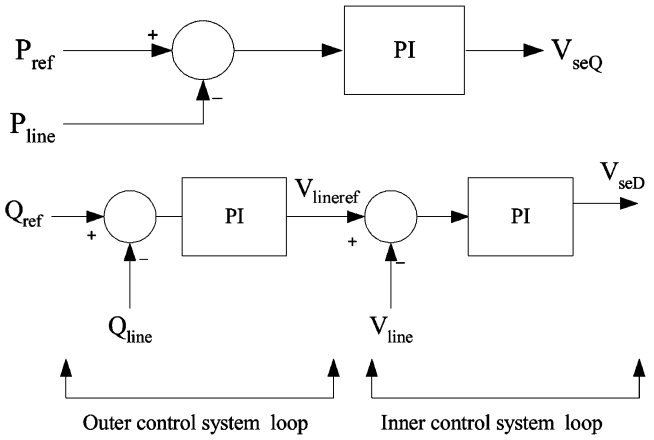

Fig. 2. Series converter real and reactive power flow control system.

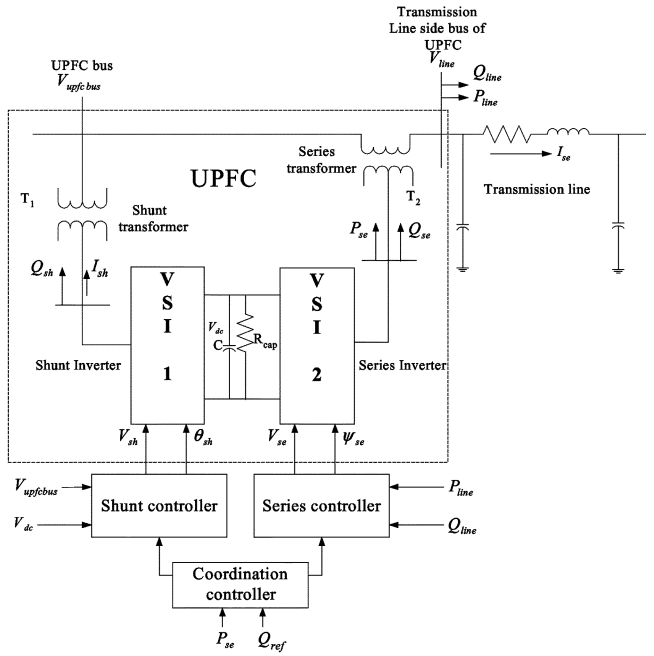

Fig. 3. UPFC connected to a transmission line.

B. Series Converter Control System

Fig. 2 shows the overall series converter control system. The transmission line real power flow $(P_{\rm line})$ is controlled by injecting a component of the series voltage in quadrature with the UPFC bus voltage $(V_{\rm se}Q)$. The transmission line reactive power $(Q_{\rm line})$ is controlled by modulating the transmission line side bus voltage reference $(V_{\rm lineref})$. The transmission line side bus voltage is controlled by injecting a component of the series voltage in-phase with the UPFC bus voltage $(V_{\rm se}D)$. The parameters of the PI controllers are given in Appendix A.

IV. Real and Reactive Power Coordination Controller

A. Real Power Coordination Controller

To understand the design of a real power coordination controller for a UPFC, consider a UPFC connected to a transmission line as shown in Fig. 3. The interaction between the series injected voltage $(V_{\rm se})$ and the transmission line current $(I_{\rm se})$ leads

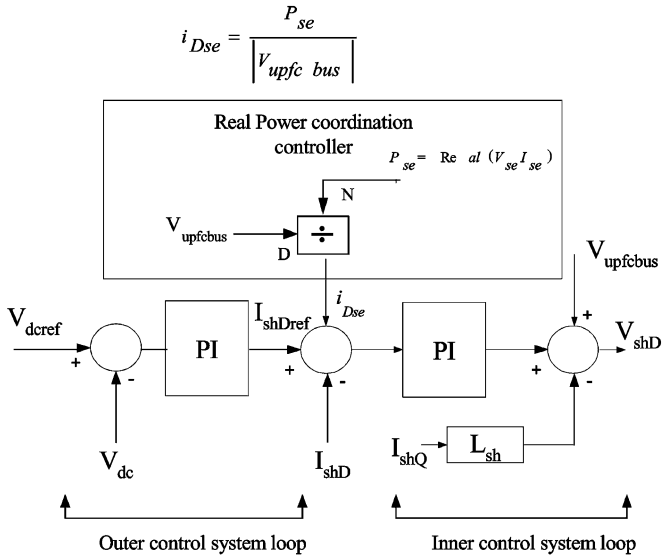

Fig. 4. D-axis shunt converter control system with real power coordination controller.

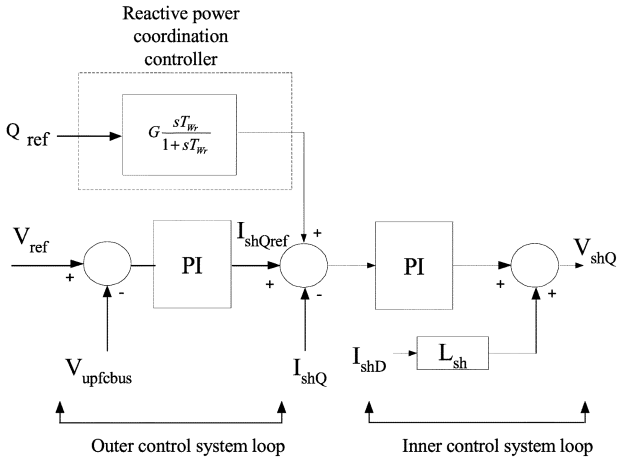

Fig. 5. Shunt converter Q-axis controller with reactive power coordination controller.

to exchange of real power $(P_{\rm se})$ between the series converter and the transmission line. The real power demand of the series converter $(P_{\rm se})$ causes the dc link capacitor voltage $(V_{\rm dc})$ to either increase or decrease depending on the direction of the real power flow from the series converter. This decrease/increase in dc link capacitor voltage $(V_{\rm dc})$ is sensed by the shunt converter controller that controls the dc link capacitor voltage $(V_{\rm dc})$ and acts to increase/decrease the shunt converter real power flow to bring the dc link capacitor voltage $(V_{\rm dc})$ back to its scheduled value. Alternatively, the real power demand of the series converter is recognized by the shunt converter controller only by the decrease/increase of the dc link capacitor voltage $(V_{\rm dc})$. Thus, the shunt and the series converter operation are in a way separated from each other. To provide for proper coordination between the shunt and the series converter control system, a feedback from the series converter is provided to the shunt converter control system. The feedback signal used is the real power demand of the series converter $(P_{\rm se})$. The real power demand of the series converter $(P_{\rm se})$ is converted into an equivalent D-axis current for the shunt converter $(i_{D\rm se})$. By doing so, the shunt converter responds immediately to a change in its D-axis current and supplies the necessary series converter real power demand. The equivalent D-axis current $(i_{D\rm se})$ is an additional input to the D-axis shunt converter control system as shown in Fig. 4. Equation (1) shows the relationship between the series converter real power demand $(P_{\rm se})$ and the shunt converter D-axis current $(i_{D\rm se})$

$$i_{D\rm se} = \frac{P_{\rm se}}{|V_{\rm upfc\ bus}|}. \tag{1}$$

The real power demand of the series converter $P_{\rm se}$ is the real part of product of the series converter injected voltage $V_{\rm se}$ and the transmission line current $I_{\rm se}$. $V_{\rm upfcbus}, i_{D\rm se}$ represent the voltage of the bus to which the shunt converter is connected and the equivalent additional D-axis current that should flow through the shunt converter to supply the real power demand of the series converter. As shown in Fig. 4, the equivalent D-axis additional current signal $(i_{D\rm se})$ is fed to the inner control system, thereby increasing the effectiveness of the coordination controller. Further, the inner control system loops are fast acting PI controllers and ensure fast supply of the series converter real power demand $(P_{\rm se})$ by the shunt converter.

B. Reactive Power Coordination Controller

The in-phase component $(V_{{\rm se}D})$ of the series injected voltage which has the same phase as that of the UPFC bus voltage, has considerable effect on the transmission line reactive power $(Q_{\rm line})$ and the shunt converter reactive power $(Q_{\rm sh})$. Any increase/decrease in the transmission line reactive power $(Q_{\rm line})$ due to in-phase component $(V_{{\rm se}D})$ of the series injected voltage causes an equal increase/decrease in the shunt converter reactive power $(Q_{\rm sh})$ [19]. In short, increase/decrease in transmission line reactive power is supplied by the shunt converter. Increase/decrease in the transmission line reactive power also has considerable effect on the UPFC bus voltage. The mechanism by which the request for transmission line reactive power flow is supplied by the shunt converter is as follows. Increase in transmission line reactive power reference causes a decrease in UPFC bus voltage. Decrease in UPFC bus voltage is sensed by the shunt converter UPFC bus voltage controller which causes the shunt converter to increase its reactive power output to boost the voltage to its reference value. The increase in shunt converter reactive power output is exactly equal to the increase requested by the transmission line reactive power flow controller (neglecting the series transformer T_2 reactive power loss). Similarly, for a decrease in transmission line reactive power, the UPFC bus voltage increases momentarily. The increase in UPFC bus voltage causes the shunt converter to consume reactive power and bring the UPFC bus voltage back to its reference value. The decrease in the shunt converter reactive power is exactly equal to the decrease in transmission line reactive power flow (neglecting the reactive power absorbed by the series transformer T_2). In this process, the UPFC bus voltage experiences excessive voltage excursions. To reduce the UPFC bus voltage excursions, a reactive power flow coordination controller has been designed. The input to the reactive power coordination controller is the transmission line reactive power reference. Fig. 5 shows the shunt converter Q-axis control system with the reactive power coordination controller.

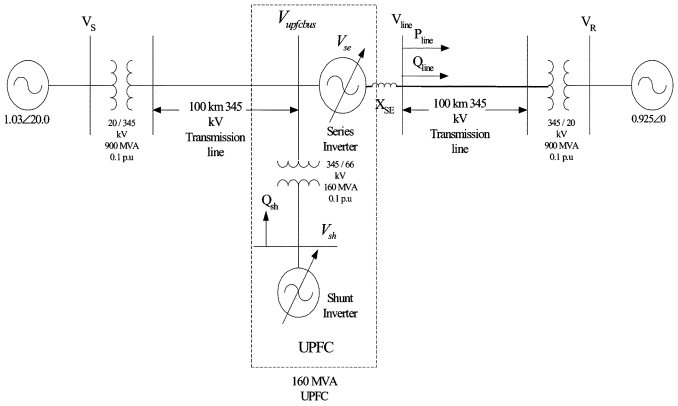

Fig. 6. Power system with UPFC.

The washout circuit represents the reactive power coordination controller. The gain of the washout circuit has been chosen to be 1.0. This is because, any increase/decrease in the transmission line reactive power flow due to change in its reference is supplied by the shunt converter. The washout time constant is designed based on the response of the power system to step changes in transmission line reactive power flow without the reactive power coordination controller.

V. UPFC Simulation Model

PSCAD-EMTDC software has been used to model the UPFC. The shunt converter has been modeled as a 4-module converter. The series converter consists of two sets of converters. One set of converter is used for the real power flow control and the other set of converter is used for the reactive power flow control. Recent advances in high voltage IGCT technology allow for higher switching frequencies with lower losses. This allows for practical implementation of PWM control [18]. The switching frequency for the converters has been chosen to be nine times the fundamental. A rating of 160 MVA has been assumed for the shunt transformer and series transformer. The UPFC parameters are given in Appendix B.

VI. Simulation Results

A. Response to Step Changes in Transmission Line Real Power Flow Reference

Fig. 6 shows the power system with UPFC considered to study the response of the power system to step changes in transmission line real power flow reference. The UPFC is located at the center of a 200 km 345 kV transmission line. The initial real power flow in the transmission line is 450 MW. At 10 s the transmission line real power reference is changed from 450 to 290 MW. At 12 s, the reference is changed from 290 to 450 MW. Plot-1 through Plot-3 of Fig. 7 shows the transmission line real power flow for step changes in its reference. Plot-2 and plot-3 are the enlarged version of plot-1 around 10 s and 12 s, respectively.

B. Response of the Power System to Step Changes in Reactive Power Flow Reference

Plot-1 through plot-8 of Fig. 8 shows the response of the power system (Fig. 6) to step changes in transmission line reactive power reference ($Q_{\rm ref}$). The initial real and reactive power flow ($P_{\rm line}, Q_{\rm line}$) in the transmission line are 290 MW and 125 MVAR, respectively. The initial shunt converter reactive power ($Q_{\rm sh}$) is 80 MVAR.

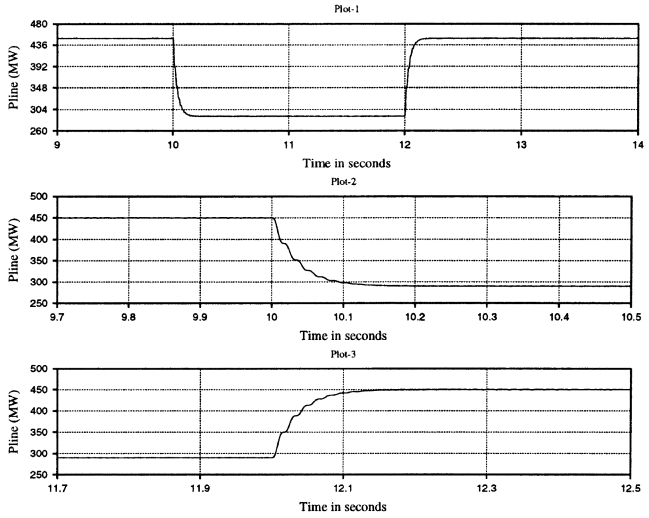

Fig. 7. Response of power system to step changes in transmission line real power reference.

Step changes of 160 MVAR in transmission line reactive power reference are conducted at 10 s and 12 s. Comparing Plot-3, Plot-4 with Plot-7 and Plot-8, respectively, it is seen that the decrease/increase in transmission line reactive power is balanced by an equal decrease/increase in shunt converter reactive power. It is seen from plot-5 of Fig. 8 that at 10 s, the UPFC bus voltage ($V_{\rm upfcbus}$) shoots to 1.05 p.u. momentarily for a step decrease of 160 MVAR in transmission line reactive power reference ($Q_{\rm ref}$). Similarly at 12 s, the UPFC bus voltage ($V_{\rm upfcbus}$) drops to 0.95 p.u. momentarily for a step increase of 160 MVAR in transmission line reactive power flow ($Q_{\rm line}$). Accordingly, the shunt converter control system senses the momentary changes in UPFC bus voltage ($V_{\rm upfcbus}$) and changes its reactive power output ($Q_{\rm sh}$) to bring the UPFC bus voltage ($V_{\rm upfcbus}$) to its reference value. The sluggish response of the shunt converter reactive power ($Q_{\rm sh}$) is due to slow change in UPFC bus voltage. The shunt converter reactive power ($Q_{\rm sh}$) changes its output with a time constant of about 80 ms ($1/5$ th of 400 ms). This information is used to design the washout time constant of the reactive power coordination controller.

C. Response of the Power System to Step Changes in Transmission Line Reactive Power Reference With Reactive Power Coordination Controller

The input to the reactive power coordination controller is the transmission line reactive power reference ($Q_{\rm ref}$). The output of the reactive power coordination controller modulates the shunt converter reactive current reference ($I_{{\rm sh}Q{\rm ref}}$). The time constant $T_{\rm Wr}$ has been chosen to be 0.5 s, which is close to the settling time for the shunt converter reactive power (Fig. 8, plot-7 and plot-8).

By doing so, the change in effective shunt converter reactive current reference ($I_{{\rm sh}Q{\rm ref}}$ + *output from reactive coordination controller*) would take a longer time to decay allowing

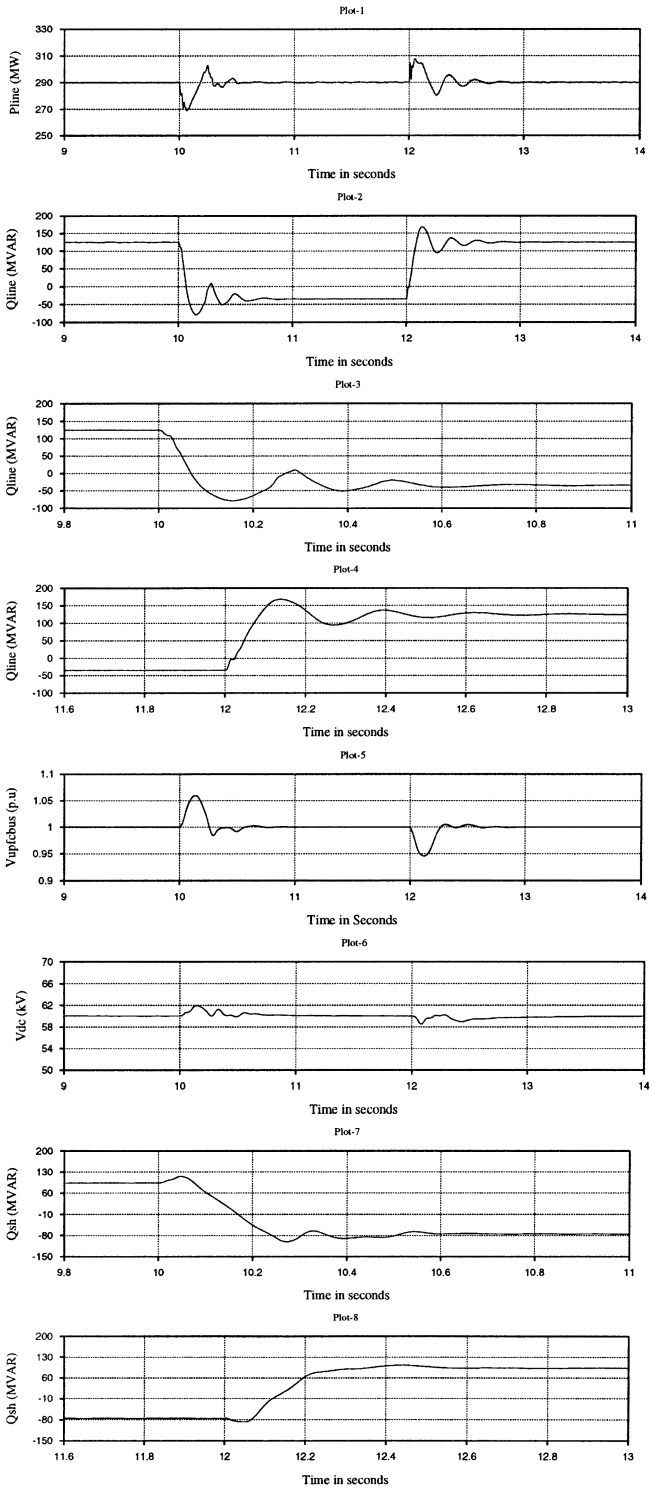

Fig. 8. Response to step change in reactive power reference.

for sufficient time for the outer loop UPFC bus voltage controller to react. This helps in reducing the UPFC bus voltage (V_{upfcbus}) excursion during step changes in transmission line reactive power reference (Q_{ref}).

Fig. 9 shows the comparison of the UPFC bus voltage (V_{upfcbus}) and transmission line reactive power with and without the reactive power coordination controller. With the reactive power coordination controller, the UPFC bus voltage excursion has reduced significantly. The impact of reactive

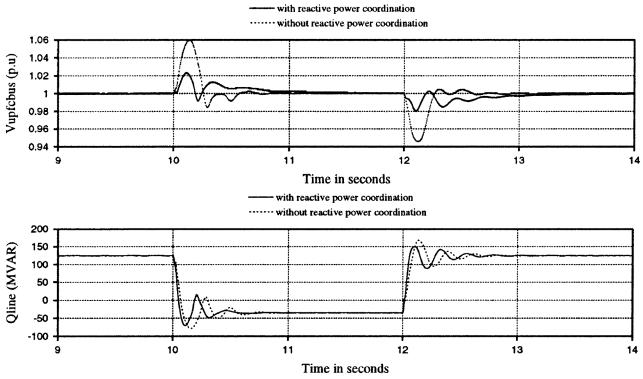

Fig. 9. Impact of reactive power coordination controller.

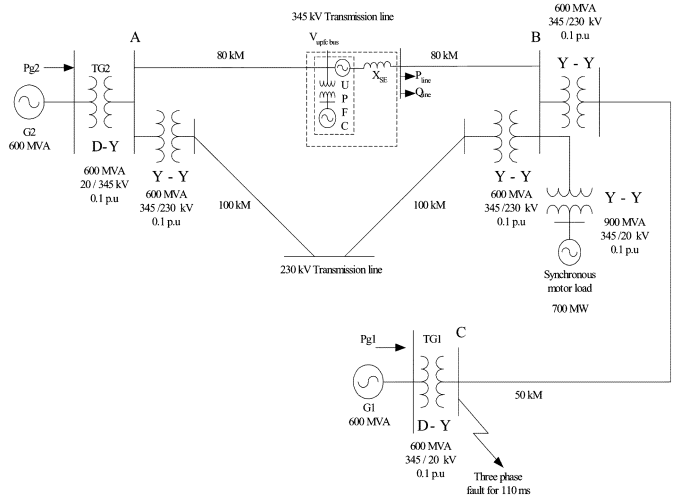

Fig. 10. Power system with UPFC.

power coordination controller on transmission line reactive power flow is minimal.

D. Effect of Real Power Coordination Controller

To study the efficacy of the real power coordination controller, a power system shown in Fig. 10 has been considered. The machines are equipped with static exciters and PSS. The generator, exciter, PSS, synchronous motor load, and UPFC parameters are given in Appendix B [21]. The total load in the power system is 700 MW. The load has been modeled as a synchronous motor. Generator G2 supplies 500 MW of power and the rest of the power is generated by G1. Generator G1 also supplies the system losses. The steady-state power flow in the 345 kV transmission line is 400 MW. The 230 kV transmission line carries 100 MW of power. The UPFC is located at the center of a 160-km 345-kV line.

The shunt converter of the UPFC controls the dc link capacitor voltage (V_{dc}) and the shunt converter reactive power. The series converter of the UPFC controls the real power flow in the transmission line (P_{line}) at 400 MW and the reactive power flow at 100 MVAR. A three-phase fault is conducted at 12 s for 50 ms at bus-B with no change in network configuration. Plot-1 and Plot-2 (enlarged version of Plot-1) of Fig. 11 shows the dc link capacitor voltage with and without the real power coordination controller. The three-phase fault causes the real power to

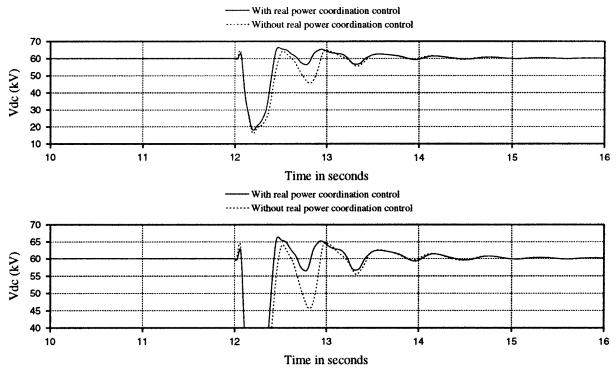

Fig. 11. Impact of real power coordination controller.

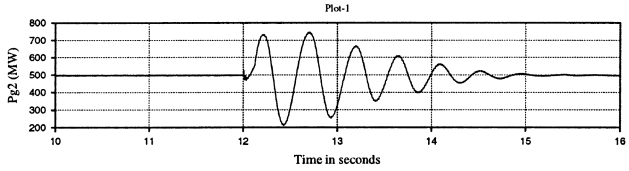

Fig. 12. Response of the power system to three-phase fault without UPFC.

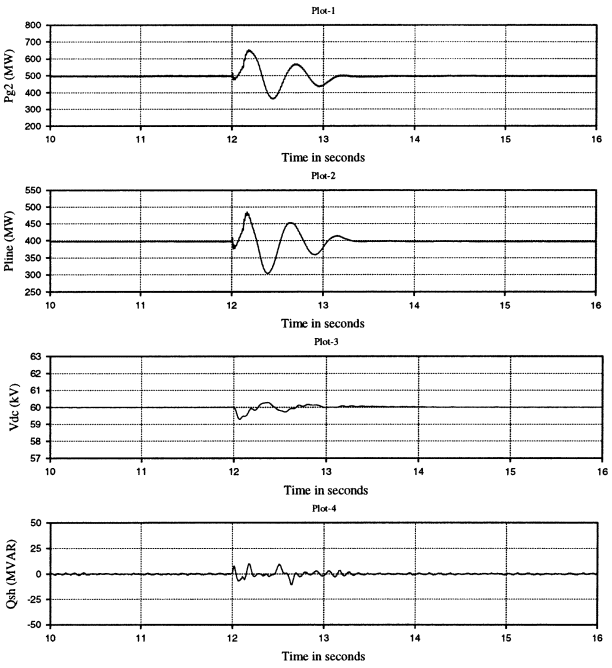

Fig. 13. Response of the power system to three-phase fault with UPFC.

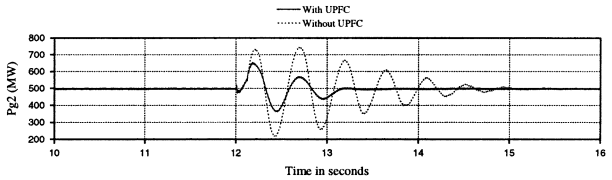

Fig. 14. Generator G2 electrical power with and without UPFC.

be generated by the UPFC leading to reduction in dc link capacitor voltage. The dc link capacitor voltage drops to about 20 kV. Following the fault removal, the dc link capacitor is charged up by the shunt converter. It is evident from plot-1 and plot-2 of Fig. 11 that the real power coordination controller has significantly improved the recovery of the dc link capacitor voltage under transient conditions. Further, the dc link capacitor voltage oscillations are well damped with real power coordination controller.

E. Power Oscillation Damping

A two-machine (G1 and G2) power system shown in Fig. 10 has been modeled in PSCAD-EMTDC to study the improvement in power oscillation damping of generator G2 using a UPFC. A three-phase fault is applied at the high voltage bus of generator G1(bus-C) at 12 s for 110 ms and removed without any change in the network configuration. Fig. 12 shows the electrical power (P_{g2}) oscillations of the generator G2 without the UPFC for the three-phase fault.

To show the improvement in power oscillation damping with UPFC, the UPFC is located at bus-A as shown in Fig. 10. In this case, the shunt converter of the UPFC controls the dc link capacitor voltage $(V_{\rm dc})$ at 60 kV and the shunt reactive power at zero. The series converter of the UPFC controls the real power flow in the transmission line $(P_{\rm line})$ at 400 MW. The reactive power flow controller has been disabled for this simulation as it does not contribute much to real power oscillation damping. Linear control analysis has been used to design the control system for the series converter [20].

Plot-1 through plot-4 of Fig. 13 shows the response of the system with UPFC for a three phase fault at bus-C for 110 ms. The generator G2 oscillations are well damped. The UPFC has regulated the dc link voltage at 60 kV, the shunt converter reactive power at zero and the transmission line real power flow to 400 MW.

Fig. 14 shows the comparison between the response of the generator G2 electrical power (P_{g2}) with UPFC and without UPFC. It is evident from Fig. 14 that the UPFC has significantly improved the damping of generator G2 power oscillations.

VII. Conclusion

This paper has presented a new real and reactive power coordination controller for a UPFC. The basic control strategy is such that the shunt converter of the UPFC controls the UPFC bus voltage/shunt reactive power and the dc link capacitor voltage. The series converter controls the transmission line real and reactive power flow. The contributions of this work can be summarized as follows.

Two important coordination problems have been addressed in this paper related to UPFC control. One, the problem of real power coordination between the series and the shunt converter control system. Second, the problem of excessive UPFC bus voltage excursions during reactive power transfers requiring reactive power coordination.

Inclusion of the real power coordination controller in the UPFC control system avoids excessive dc link capacitor voltage excursions and improves its revovery during transient conditions. PSCAD-EMTDC simulations have been conducted to verify the improvement in dc link voltage excursions during transient conditions.

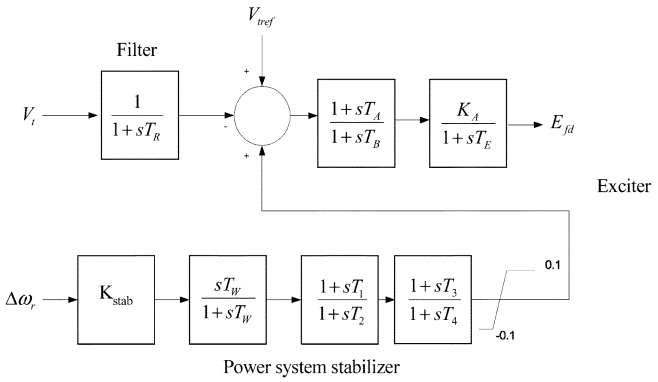

Fig. 15 Exciter and power system stabilizer.

Inclusion of reactive power coordination controller helps in significantly reducing UPFC bus voltage excursions during reactive power transfers. The effect on transmission line reactive power flow is minimal.

PSCAD-EMTDC simulations have shown the improvement in power oscillation damping with UPFC.

APPENDIX

A. Series Converter Control Parameters

1) Transmission line real power flow controller parameters

$$K_p = 0.1 \quad K_I = 4.0.$$

2) Transmission line reactive power flow controller parameters:
   a) Outer loop controller: $K_p = -0.1 \;\; K_I = -1.0.$
   b) Inner loop controller: $K_p = 0.15 \;\; K_I = 25.0.$

B. Power System Parameters

1) Generator parameters

$$L_{\mathrm{adu}} = 1.6 \quad L_{\mathrm{aqu}} = 1.5 \quad ll = 0.2 \quad L_{\mathrm{ad}} = 0.835\, L_{\mathrm{adu}}$$
$$L_{\mathrm{aq}} = 0.835\, L_{\mathrm{aqu}} \quad L_{\mathrm{fd}} = 0.106\,67 \quad r_{\mathrm{fd}} = 0.000\,565\,8$$
$$L_{1d} = 0.1 \quad r_{1d} = 0.017\,68 \quad L_{1q} = 0.456\,52$$
$$r_{1q} = 0.012\,97 \quad L_{2q} = 0.058\,33 \quad r_{2q} = 0.021\,662$$
$$H(1) = 3.15 \quad H(2) = 3.5.$$

2) UPFC parameters
   Dc link capacitor $= 3000\ \mu$F.
   Shunt converter transformer is rated at
   160 MVA, 345/66 kV, $X_{\mathrm{sh}} = 0.2$ p.u.
   Series converter transformer is rated at 160 MVA.
   38.1/66 kV, $X_{\mathrm{SE}} = 0.04$ p.u.

3) Exciter and power system stabilizer parameters (see Fig. 15)

$$K_{\mathrm{stab}} = 9.5 \quad T_W = 10.0 \quad T_1 = 0.05 \quad T_2 = 0.02$$
$$T_3 = 3.0 \quad T_4 = 5.4 \quad T_R = 0.02$$
$$K_A = 200.0 \quad T_A = 1.5 \quad T_B = 1.0 \quad T_E = 0.02.$$

4) Synchronous motor load parameters:
   a) Rating: 900 MVA, 20 kV.
   b) Parameters

$$X_{S1} = 0.14 \quad X_{\mathrm{MDO}} = 1.445 \quad X_{23O} = 0.0$$
$$X_{3D} = 0.0437 \quad X_{2D} = 0.2004 \quad X_{\mathrm{MQ}} = 0.91$$
$$X_{2Q} = 0.106 \quad R_{S1} = 0.0025 \quad R_{2D} = 0.000\,43$$
$$R_{3D} = 0.0051 \quad R_{2Q} = 0.008\,42 \quad H = 1.0.$$

REFERENCES

[1] L. Gyugyi, C. D. Schauder, S. L. Williams, T. R. Reitman, D. R. Torgerson, and A. Edris, "The unified power flow controller: A new approach to power transmission control," *IEEE Trans. Power Delivery*, vol. 10, pp. 1085–1097, Apr. 1995.

[2] C. D. Schauder, L. Gyugyi, M. R. Lund, D. M. Hamai, T. R. Rietman, D. R. Torgerson, and A. Edris, "Operation of the unified power flow controller (UPFC) under practical constraints," *IEEE Trans. Power Delivery*, vol. 13, pp. 630–636, Apr. 1998.

[3] K. K. Sen and E. J. Stacey, "UPFC-UnifiedPower flow controller: Theory, modeling, and applications," *IEEE Trans. Power Delivery*, vol. 13, pp. 1453–1460, Oct. 1999.

[4] B. A. Renz, A. S. Mehraben, C. Schauder, E. Stacey, L. Kovalsky, L. Gyugyi, and A. Edris, "AEP unified power flow controller performance," *IEEE Trans. Power Delivery*, vol. 14, pp. 1374–1381, Oct. 1999.

[5] P. K. Dash, S. Mishra, and G. Panda, "A radial basis function neural netwrok controller for UPFC," *IEEE Trans. Power Syst.*, vol. 15, pp. 1293–1299, Nov. 2000.

[6] ——, "Damping multimodal power system oscillation using a hybrid fuzzy controller for series connected FACTS devices," *IEEE Trans. Power Syst*, vol. 15, pp. 1360–1366, Nov. 2000.

[7] Z. Huang, Y. Ni, F. F. Wu, S. Chen, and B. Zhang, "Appication of unified power flow controller in interconnected power systems-modeling, interface, control strategy and case study," *IEEE Trans. Power Syst*, vol. 15, pp. 817–824, May 2000.

[8] Y. Morioka, Y. Mishima, and Y. Nakachi, "Implementation of unified power flow controller and verification of transmission capability improvement," *IEEE Trans. Power Syst*, vol. 14, pp. 575–581, May 1999.

[9] P. C. Stefanov and A. M. Stankovic, "Modeling of UPFC operation under unbalanced conditions with dynamic phasors," *IEEE Trans. Power Syst.*, vol. 17, pp. 395–1403, May 2002.

[10] H. F. Wang, "A unified model for the analysis of facts devices in damping power system oscillations part I: Single machine infinite-bus power systems," *IEEE Trans. Power Delivery*, vol. 12, pp. 941–946, Apr. 1997.

[11] ——, "A unified model for the analysis of facts devices in damping power system oscillations part II: Multi-machine power syetms," *IEEE Trans. Power Delivery*, vol. 13, pp. 1355–1361, Oct. 1998.

[12] ——, "A unified model for the analysis of facts devices in damping power system oscillations part III: Unified power flow controller," *IEEE Trans. Power Delivery*, vol. 15, pp. 978–983, July 2000.

[13] R. Mihilac, P. Zunko, and D. Povh, "Improvement of transient stability using unified power flow controller," *IEEE Trans. Power Delivery*, vol. 11, pp. 485–492, Jan. 1996.

[14] K. R. Padiyar and A. M. Kulkarni, "Control design and simulations of unified power flow controller," *IEEE Trans. Power Delivery*, vol. 13, pp. 1348–1354, Oct. 1998.

[15] I. Papic, P. Zunko, and D. Povh, "Basic control of unified power flow controller," *IEEE Trans. Power Syst.*, vol. 12, pp. 1734–1739, Nov. 1997.

[16] C. Schauder, "Vector analysis and control of advanced static var compensators," in *Proc. Inst. Elect. Eng. C*, vol. 140, 1993, pp. 299–306.

[17] S. Kannan, S. Jayaram, and M. M. A. Salama, "Design of a de-coupled controller for a shunt converter: Control design and performance," in *Proc. 32nd North American Power Symp.*, Waterloo, ON, Canada, Oct. 2000, pp. 8–13.

[18] P. K. Steimer, H. E. Gruning, E. Carroll, S. Klaka, and S. Linder, "IGCT: A new emerging technology for high power, low cost converters," in *Proc. IEEE Industrial Applications Society, Annual Meeting*, New Orleans, LA, Oct. 1997.